

Enhancement of Seismic Capacity of Masonry Shear Walls by Use of Reinforced Concrete-Gap-Element and Experimental Study Using Pseudo-Dynamic Substructure-Tests



E. Fehling

Prof. Dr.- eng. University of Kassel, Germany

E. Aldoghaim

Dr.- eng. University of Kassel, Germany

SUMMARY:

By building failures caused by earthquake worldwide each year, many people are injured or killed. The best way to prevent this is to improve our understanding of the phenomenon and to develop improved regulations of earthquake-resistant construction. The state of knowledge on masonry structures in this context is far less developed than in other construction designs such as concrete, steel and timber structures. Against the background, that most residential buildings in central Europe are built of unreinforced masonry, this is of particular importance. For this reason, a new method has been proposed for improving the behavior of masonry walls by using reinforced concrete beams with corner notches (Concrete-Gap-Element), which can be applied at low cost.

In this paper we show how masonry walls with integrated reinforced concrete beams (bottom only, top and bottom) behave as a typical bearing walls in a masonry building. Therefore, pseudo-dynamic tests were performed on brick masonry walls with and without Concrete-Gap-Element in different configurations as a substructure of a 2-Story house at the laboratory for Structural Engineering of the University of Kassel.

Keywords: Gap-Element, Seismic Capacity, Pseudo-Dynamic, Substructure-Test.

1. INTRODUCTION

On way to improve the behavior of slender masonry walls in case of an earthquake can be achieved by using a Concrete-Gap-Element, which has notches in cross section at each side and help to avoid early failure of masonry due to stress concentrations in corners. Figure 1.1 explains the main idea of the Concrete-Gap-Element and the way of loading of masonry walls that in most cases leads to a high exploitation of the shear capacity.

During increase of the bending moments with shear forces, the eccentricity of the normal force in the critical cross section becomes significant. This in turn leads to a reduction of the length of the compression zone in unreinforced walls with high concentration of normal stresses and shear stresses. In order to solve this problem, reinforced Concrete-Gap-Elements, enabling the transfer of the capacity design concept to unreinforced masonry have been proposed. It was investigated, how masonry walls with bottom only or top and bottom bearing concrete beam behave in typical houses in comparison to plain masonry walls without any notched concrete bearing beams.

Shaking table tests [Nejati, 2005] have shown the suitability of this concept in the case of an earthquake. For experimental verification of the application of Gap-Element, 10 pseudo-dynamic tests were carried out on masonry walls. While the masonry wall of the ground floor has been tested in the laboratory in full scale, the rest of the masonry building has been simulated numerically at the same time. On top of the wall, two hydraulic cylinders apply vertical loads while the third one applies load in horizontal direction. Corresponding to the three degrees of freedom at the top of the wall, a dynamic condensation was carried out depending on the three main vibration forms.

This article shows the experimental technique, significant results in term of the redistribution of normal forces, measured force-displacement hystereses and the possible increase of the earthquake resistance of the masonry wall by applying reinforced Concrete-Gap-Elements.

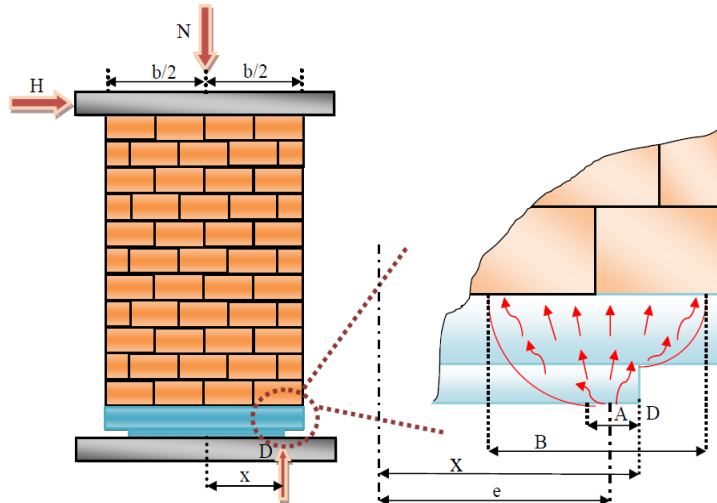


Figure 1.1. Concrete-Gap-Element in masonry wall

2. PSEUDO-DYNAMIC SUBSTRUCTURE-TEST-TECHNIQUE

2.1. Basics

In Pseudo-Dynamic Substructure-Testing, the system is normally divided into two parts. The first substructure is the experimental part and the second one is the numerical substructure. This method enables to simulate large structures under dynamic loading by testing only a part of the system (bearing wall in Figure 2.1) experimentally, while all the rest of the system and inertial effects can be described by mathematical simulation (Method of Pseudo-Dynamic Testing PDT). The family-house as investigated within the framework of the ESECMaSE Project [Anthoine, 2007] in the Joint Research Center Ispara, Italy (JRC) was selected here for the experimental program described in the following.

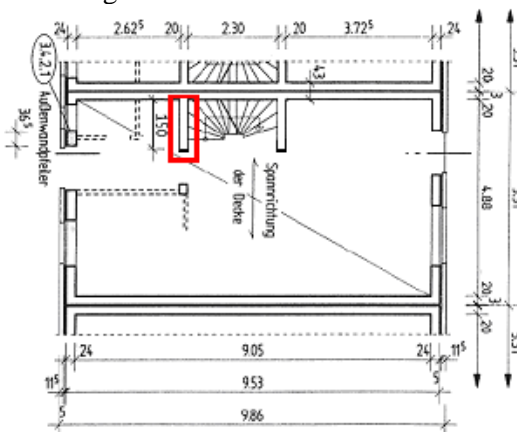


Figure 2.1. Top-View the entire masonry building at JRC Ispara, [2].

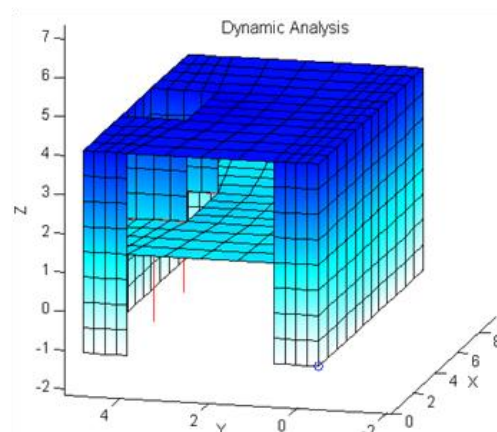


Figure 2.2. The FE-Model of the entire masonry building, [Fehling & Aldoghaim, 2011]

In the finite element model the main masonry shear wall on the ground floor was represented through a special T-element, which transfers the behavior of the masonry shear wall tested in reality (displacements, rotations, and nodal forces) into the FE-Model. In the substructure-technique, the stiffness of the entire structure is required in each step within the equilibrium iteration of each time step. This would lead to long computational and experimental time. To solve this problem, the entire system is transformed on the basis of the selected most important three vibration modes of the structure from the modal matrix according to equation (2.1) in a modal coordinate system, see Figure 2.3. The differential equations now are solved in the new coordinate system using the PDT-algorithm

for these three vibration modes. In the ESECMaSE Project, an algorithm using the implicit α -method for solving dynamic equation with one degree of freedom was implemented by Aldoghaim [Fehling et al., 2011]. Here, this algorithm is extended to solve the three decoupled dynamic equations iteratively.

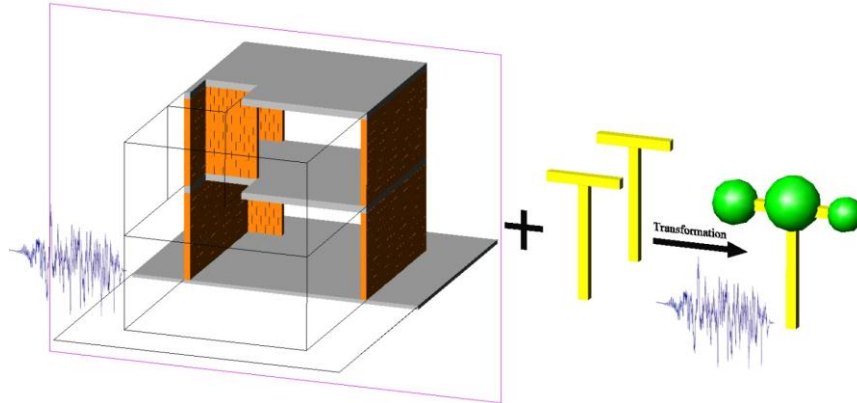


Figure 2.3. Transformation of the system in the modal coordinate system [Fehling & Aldoghaim, 2011].

$$\begin{aligned} [\bar{M}]_{n \times n} \cdot \{\ddot{\bar{u}}\}_{n \times 1} + [C]_{n \times n} \cdot \{\dot{\bar{u}}\}_{n \times 1} + [\bar{K}_{SB} + \bar{K}_W]_{n \times n} \cdot \{\bar{u}\}_{n \times 1} &= a_g \cdot [\bar{M}]_{n \times n} \xrightarrow{\text{Transformation}} \\ [\mu]_{3 \times 3} \cdot \{\ddot{\bar{q}}\}_{3 \times 1} + [\Delta]_{3 \times 3} \cdot \{\dot{\bar{q}}\}_{3 \times 1} + [\bar{\gamma}_{SB} + \bar{\gamma}_W]_{3 \times 3} \cdot \{\bar{q}\}_{3 \times 1} &= \{\bar{F}_r\}_{3 \times 1} \end{aligned} \quad (2.1)$$

Here:

$\mu = \Phi_{3 \times n}^T \cdot M_{n \times n} \cdot \Phi_{n \times 3}$	is the mass matrix in the modal coordinate system,
$\Phi_{n \times 3}$	is the modal matrix from three selected vibration modes,
$\Delta = \Phi_{3 \times n}^T \cdot C_{n \times n} \cdot \Phi_{n \times 3}$	is the damping matrix in modal coordinates,
$\gamma_{SB} = \Phi_{3 \times n}^T \cdot K_{SB(n \times n)} \cdot \Phi_{n \times 3}$	is the stiffness matrix of the sub-structure in the modal coordinate system,
$\gamma_w = \Phi_{3 \times n}^T \cdot K_{w(n \times n)} \cdot \Phi_{n \times 3}$	is the stiffness matrix of the tested wall in the modal coordinate system,
q, \dot{q}, \ddot{q}	are the displacement, velocity and acceleration vectors in the modal coordinate system,
F_r	are the inertial forces in the modal coordinate system.

The three selected vibration modes were determined so that they lead to both the maximum horizontal displacement and rotation as well as the vertical displacement of the top wall (represented by the T-Element). To examine the influence of neglecting other vibration modes, all possible combinations of any three modal forms were arranged in groups. The response of the structure was calculated for these combinations in the PDT-algorithm for the linear-elastic case. It could be observed, that the displacements from the selected combination of the three vibration modes are 10-time greater than the displacements from any other combination.

2.2. Non-Linear Behavior of the Main Wall

The substructure in FE-Model was simulated as linear-elastic, therefore it can be noted in the crossing area between the tested main shear wall (wall near stairs, length 1,5 m) and the perpendicular stair wall that during the vibration of the building, a tensile force in the numerically simulated stair wall can arise. In reality, this tensile force cannot occur in the masonry building because of gapping between the concrete slab and the top of the wall. In order to solve this problem and to perform our test close to reality, a bar finite element was implemented into the numerical model, see Figure 2.4. This bar element must produce a vanishing overall stiffness together with the stair wall due to elongation, so that in total no tensile force arises.

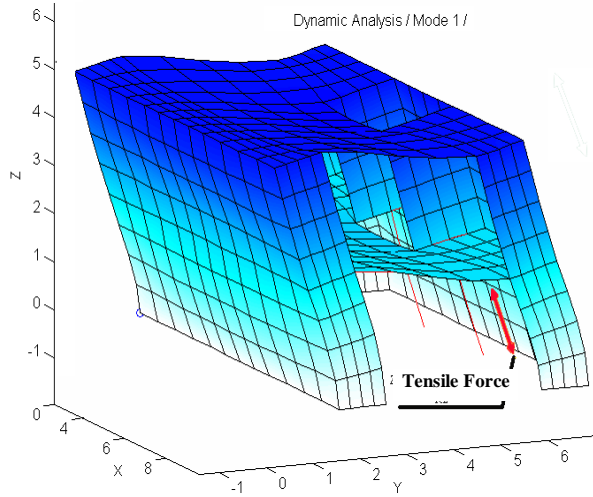


Figure 2.4-a. Tensile force in stair wall.

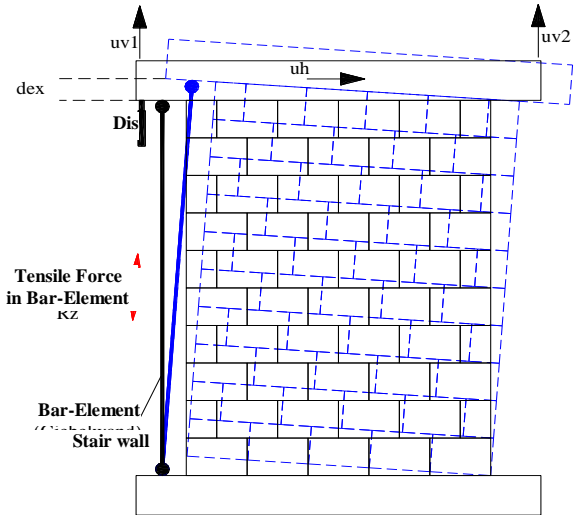


Figure 2.4-b. Tensile force in simulated bar-element.

The tensile force $R_{z,u}$ to be compensated can be calculated easily in the physical coordinate system according to equation (2.2) as follows:

$$R_{z,u} = \frac{EA}{H} \cdot d_{ex} \quad (2.2)$$

Here :

- E is the elastic modulus of the masonry stair wall
- A is the effective cross section of the stair wall in the crossing area
- H is the height of the ground floor of the masonry structure
- d_{ex} is the vertical displacement measured at the left top of the wall during the test.

Because the test is performed in the modal coordinate system, the tensile force $R_{z,u}$ must be transformed with respect of the three selected vibration modes in the modal coordinate system according to equation (2.3) and incorporated into PDT-algorithm.

$$R_{z,q} = [\varphi_1 \quad \varphi_2 \quad \varphi_3]^T \cdot \begin{bmatrix} k_{1,1} & k_{1,2} & k_{1,3} \\ k_{2,1} & k_{2,2} & k_{2,3} \\ k_{3,1} & k_{3,2} & k_{3,3} \end{bmatrix} \cdot [\varphi_1 \quad \varphi_2 \quad \varphi_3] \quad (2.3)$$

$[\varphi_1 \quad \varphi_2 \quad \varphi_3]^T$ is the transformation factor, which is obtained from the selected three vibration modes at the three nodes of the T-element from modal matrix.

The square 3x3 matrix is the stiffness of the simulated bar-element in the physical coordinate system.

In case of compression loading of the masonry stair wall, the stiffness of the bar-element must to be set zero in order to avoid a doubling of the compression force.

3. EXPERIMENTAL STUDIES ON MASONRY WALLS

3.1. Arrangement of the Concrete-Gap-Element in Masonry Wall

The Gap-Element was introduced as an innovative element which can be made of concrete or another sufficiently resistant material . The Concrete-Gap-Element can be installed in a masonry wall in the first or/and in the last wall layer of a building instead of a row of masonry units, see Figure 3.1.

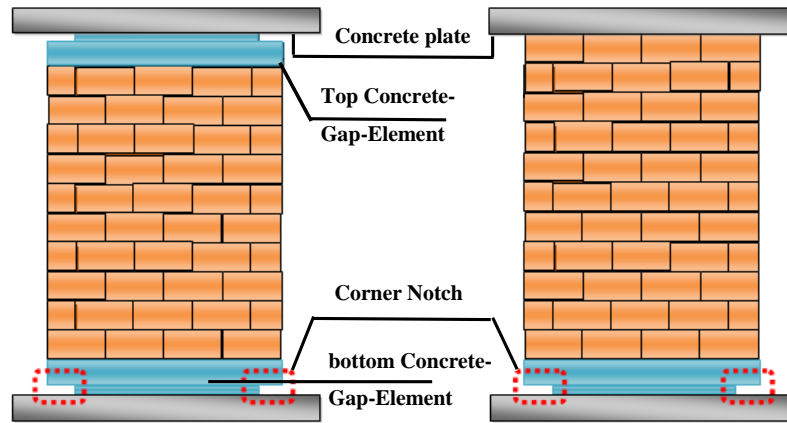


Figure 3.1-a. Masonry wall with Top and bottom Concrete-Gap-Element

Figure 3.1-b. Masonry wall with bottom Concrete-Gap-Element

In practice, the Gap-Element can be easily connected with use of normal mortar on the concrete slab. The ease of manufacture and application of the Concrete-Gap-Element in masonry walls provide a cheap and simple method for improving the seismic capacity of a masonry building in practice.

3.2. Test Program

To assess the effect of different wall length l , different vertical stress σ_v and the influence of reinforced concrete-gap-element on the shear capacity of brick masonry walls, 10 wall-tests in framework of the research project AIF were carried out, [Fehling & Aldoghaim, 2011]. The boundary conditions of the wall during the pseudo-dynamic wall test were simulated as if the wall would be located in the above mentioned typical masonry house. This means, that the influence of the expected increase of the normal force due to rocking of the wall on the behavior of the masonry wall can be taken into account in the test. The tests are intended to show the behavior of the masonry structure with Gap-Element in comparison to conventional brick masonry building without Gap-Element. Table 3.1 contains the test program with relevant parameters of the test walls. The following kinds of masonry units were used for manufacturing of masonry walls:

- Opti 2-TSQ = Opti 2- TS Quadrat/ HLZ-Plan-12-0.9-9DF, [Allgemeine Bauaufsichtliche Zulassung , 2008].
- Plan T 500 = Planelement T 500/ Z-17.1-706, [Allgemeine Bauaufsichtliche Zulassung , 2009].
- Plan T 10 = Planelement T 10/ Z-17.1-889/ 0,7 N/mm², [Allgemeine Bauaufsichtliche Zulassung , 2011].

Table 3.1. Overview of the pseudo-dynamic wall tests program.

Nr.	Masonry Wall	Masonry unit	d [mm]	h [mm]	l [mm]	f_c [N/mm ²]	σ_v [N/mm ²]	Gap-Element	Spectrum
1	PSD-OptiTSQ-200-100-UO-CS	Opti 2-TSQ	175	2500	2000	5,07	0,29	Top / Bottom	C-S
2	PSD-OptiTSQ-150-100-UO-CS	Opti 2-TSQ	175	2500	1500	5,07	0,38	Top / Bottom	C-S
3	PSD-OptiTSQ-200-100-N-CS	Opti 2-TSQ	175	2500	2000	5,07	0,29	No	C-S
4	PSD-OptiTSQ-150-100-N-CS	Opti 2-TSQ	175	2500	1500	5,07	0,38	No	C-S
5	PSD-OptiTSQ-200-100-U-CS	Opti 2-TSQ	175	2500	2000	5,07	0,29	Bottom	C-S
6	PSD-T500-200-100-UO-CS	Plan T 500	175	2500	2000	5,6	0,29	Top / Bottom	C-S
7	PSD-T10-200-100-UO-CS	Plan T 10	300	2500	2000	3,6	0,25	Top / Bottom	C-S
8	PSD-T10-200-100-U-CS	Plan T 10	300	2500	2000	3,6	0,25	Bottom	C-S
9	PSD-OptiTSQ-200-100-UO-CR	Opti 2-TSQ	175	2500	2000	5,07	0,29	Top / Bottom	C-R
10	PSD-OptiTSQ-200-200-UO-CS	Opti 2-TSQ	175	2500	2000	5,07	0,58	Top / Bottom	C-S

To create the top and bottom horizontal joints and the horizontal joints between the concrete-gap-element and the unit layers, a normal mortar (Type M10) was used while for other bed joints of the wall a thin mortar was set.

The loads on the wall were applied as displacements controlled by three hydraulic cylinders. The ground acceleration time histories were consistent with the spectral range of CS and CR according to German code 4149 and German Annex to EN 1998-1, see Figure 3.2 a and b.

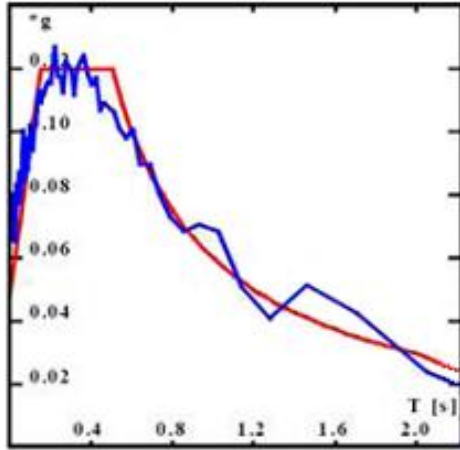


Figure 3.2-a. Elastic response spectra of acceleration time history C-S, [Anthoine, 2007].

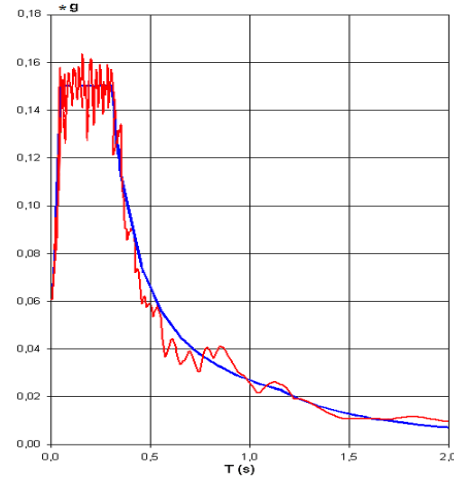


Figure 3.2-b. Elastic response spectra of acceleration time history C-R, [Fehling & Aldoghaim, 2011].

3.3. Analysis and Results of the Wall Tests

The factored input acceleration time history in experiment was increased until failure of the brick masonry wall or to reach the safety limit of the test setup. Table 2 shows both the horizontal force at the onset of crack in the wall H_E in the tension and compression direction of the horizontal-acting hydraulic cylinder and the maximum horizontal force of the masonry wall H_u . The maximum and minimum vertical force N are also listed in table 3.2. Furthermore, here are the ratio between the failure force to first crack force and the ratio of maximum horizontal shear force presented to the corresponding vertical force. In the table also, the maximum achieved horizontal displacements du_1 and du_2 of the test wall shown in both directions.

Table 3.2. The maximum failure force with corresponding normal force

Nr.	Masonry Wall	First Crack Force H_E [kN]		Failure force H_B [kN]	Vertical Force N [kN]		d_{u1} [mm]	d_{u2} [mm]	H_B / H_E [-]	H_B / N [-]	max $a_g \cdot S$ [m/sec ²]	Failure Mode
		Compression	Tension		Compression	Tension						
1	PSD-OptiTSQ-200-100-UO-CS	-100	+95	-140	-240	-222	-11,35	+10,36	1,40	0,58	0,42 g	G+Z
2	PSD-OptiTSQ-150-100-UO-CS	-65	+52	-90	-255	-216	-17,45	+20,16	1,38	0,35	0,38 g	Z
3	PSD-OptiTSQ-200-100-N-CS	-74	+74	-90	-174	-171	-6,51	+5,83	1,21	0,52	0,28 g	G
4	PSD-OptiTSQ-150-100-N-CS	-54	+52	-74	-180	-147	-7,01	+6,58	1,37	0,41	0,22 g	Z
5	PSD-OptiTSQ-200-100-U-CS	-75	+86	-112	-221	-184	-10,35	+10,21	1,49	0,51	0,38 g	Z+G
6	PSD-T500-200-100-UO-CS	-68	+55	-99	-209	-222	-11,54	+13,32	1,46	0,47	0,42 g	G
7	PSD-T10-200-100-UO-CS	-80	+80	-95	-206	-200	-9,41	+9,18	1,20	0,46	0,36 g	G
8	PSD-T10-200-100-U-CS	-79	+79	-95	-230	-240	-12,12	+10,84	1,20	0,41	0,32 g	G
9	PSD-OptiTSQ-200-100-UO-CR	-82	+80	-115	-249	-205	-10,15	+7,71	1,40	0,46	0,38 g	G+Z
10	PSD-OptiTSQ-200-200-UO-CS	-93	+69	-128	-312	-280	-11,89	+12,03	1,38	0,41	0,42 g	G+Z

An overview of the results in term of carrying capacity is in Figure 3.3. For this illustration, a non-dimensional wall factor k_w' was introduced from Stürz [Stürz, 2011], which comprises the utilization of the masonry wall in terms of normal force $\alpha = \sigma_v / f_k$ and the ratio of the wall length l_w' to wall height h_w .

$$k_w' = \frac{\sigma_v}{f_k} \cdot \frac{l_w'}{h_w} \quad (3.1)$$

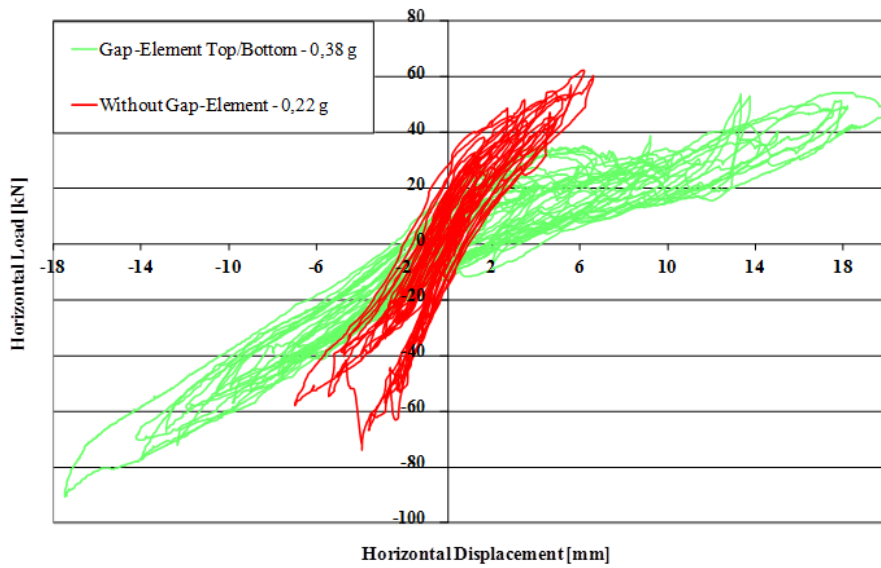


Figure 3.4-b. Effect of Gap-Element on the behavior of the wall, $l_w = 1,5$ m, [Fehling & Aldoghaim, 2011].

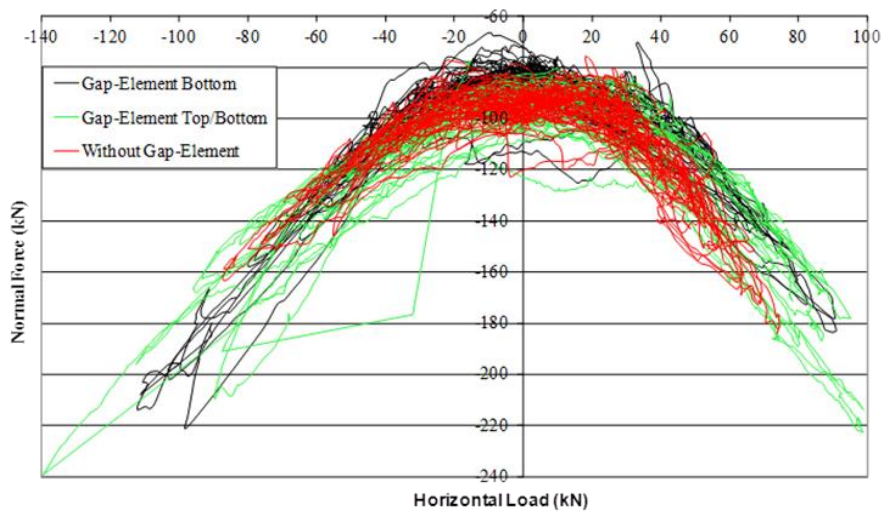


Figure 3.5-a. Development of the normal force, $l_w = 2,0$ m, [Fehling & Aldoghaim, 2011].

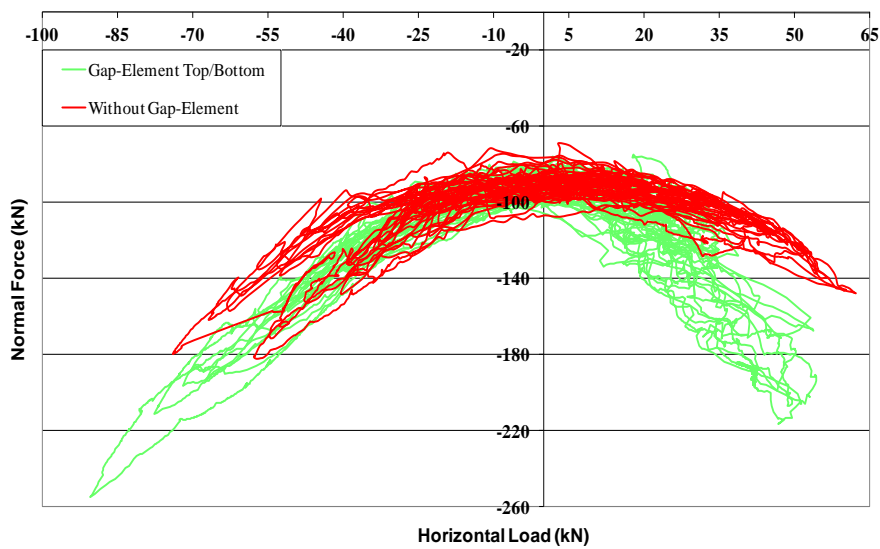


Figure 3.5-b. Development of the normal force, $l_w = 1,5$ m, [Fehling & Aldoghaim, 2011].

In the masonry walls with length $l_w = 2$ m, there is no wide difference in the response of the masonry wall (period of horizontal vibration) by existence of one or two concrete-gap-elements (Bottom only or Top and Bottom). On the other hand, the masonry walls with shorter length ($l_w = 1,5$ m) show clearly a difference in the response of the wall when two gap-elements are used (Top and Bottom) compared with one gap-element (only Bottom). For the short masonry walls with gap-element, the maximal possible ground acceleration was $a_g \cdot S = 0,38$ g and without gap-element $a_g \cdot S = 0,22$ g. so, there is 72,7% increasing in the seismic capacity of the masonry walls, see Figure 3.6. It should be noted, that the maximum possible ground acceleration $a_g \cdot S = 0,22$ g of the reference test matches very well with the results on entire houses from the Ispra tests [Anthoine & Capéran. 2008].

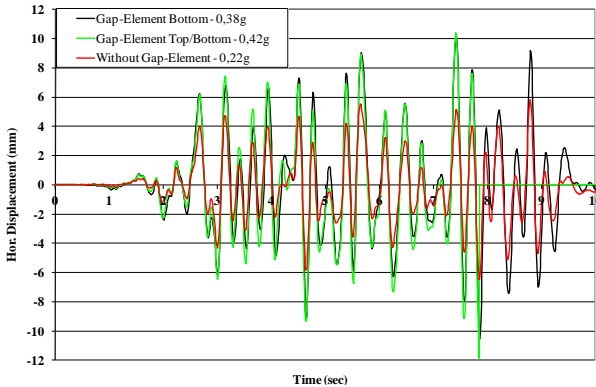


Figure 3.6-a. Horizontal displacement – Time history response of masonry wall, $l_w = 2,0$ m. [Fehling & Aldoghaim, 2011]

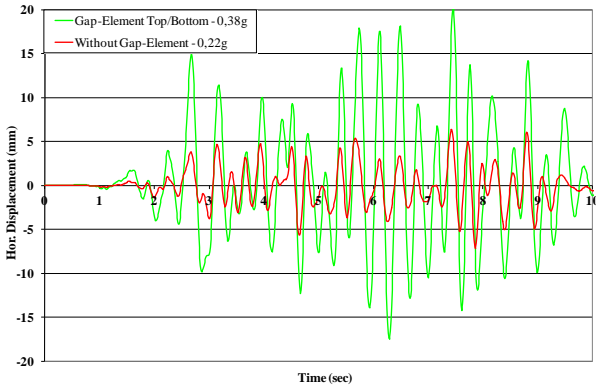


Figure 3.6-b. Horizontal displacement - Time history response of masonry wall, $l_w = 1,5$ m for maximum possible input acceleration, [Fehling & Aldoghaim, 2011].

An overview of the effect of the arrangement of one or two concrete-gap-elements on the maximum possible ground acceleration from masonry walls is given in Figure 3.7. The inclination $\tan \theta$ of the resultant force at the maximum horizontal force can be adopted from Figure 3.8.

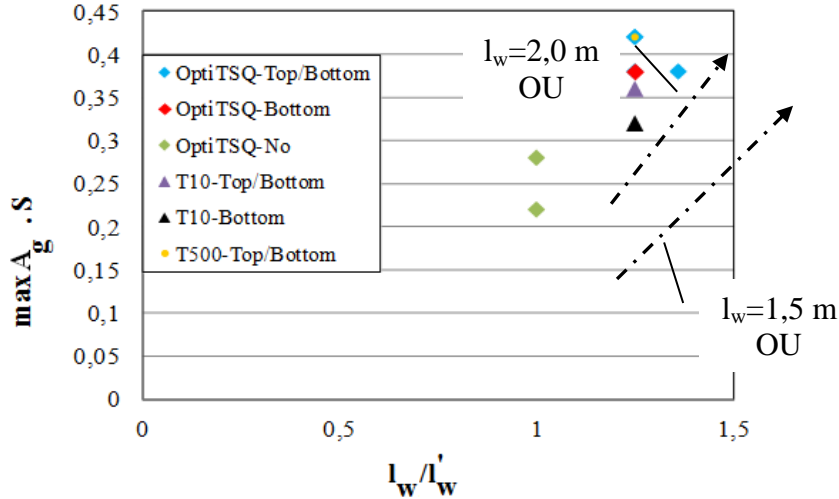


Figure 3.7. Overview of the maximum possible input ground acceleration, [Fehling & Aldoghaim, 2011].

